

REM: Routing Entropy Minimization for Capsule Networks

Riccardo Renzulli
University of Turin
Computer Science Department
riccardo.renzulli@unito.it

Enzo Tartaglione
LTCI, Télécom Paris
Institut Polytechnique de Paris
enzo.tartaglione@telecom-paris.fr

Marco Grangetto
University of Turin
Computer Science Department
marco.grangetto@unito.it

Abstract

Capsule Networks ambition is to build an explainable and biologically-inspired neural network model. One of their main innovations relies on the routing mechanism which extracts a parse tree: its main purpose is to explicitly build relationships between capsules. However, their true potential in terms of explainability has not surfaced yet: these relationships are extremely heterogeneous and difficult to understand.

This paper proposes REM, a technique which minimizes the entropy of the parse tree-like structure, improving its explainability. We accomplish this by driving the model parameters distribution towards low entropy configurations, using a pruning mechanism as a proxy. We also generate static parse trees with no performance loss, showing that, with REM, Capsule Networks build stronger relationships between capsules.

1. Introduction

Capsule Networks (CapsNets) [6,9,21] were recently introduced to overcome the shortcomings of Convolutional Neural Networks (CNNs). CNNs loose the spatial relationships between its parts because of max pooling layers, which progressively drop spatial information [21]. Furthermore, CNNs are also commonly known as “black-box” models: most of the techniques providing interpretation over the model are *post-hoc*: they produce localized maps that highlight important regions in the image for predicting objects [22]. CapsNets attempt to preserve and leverage an image representation as a hierarchy of parts, *carving-out* a parse tree from the networks. This is possible thanks to the iterative routing mechanism [21] which models the connections between capsules. This can be seen as a par-

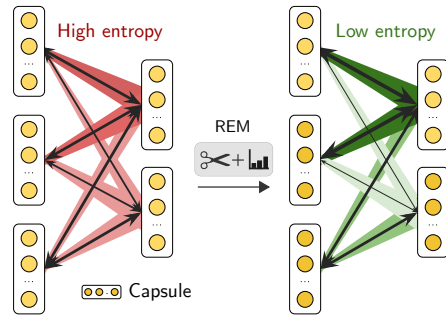


Figure 1. With REM, a Capsule Network builds stronger relationships with lower entropy between capsules.

allel attention mechanism, where each active capsule can choose a capsule in the layer above to be its parent in the tree [21]. Therefore, CapsNets can produce explainable representations encoded in the architecture itself [21] yet can be still successfully applied to a number of applicative tasks [1, 17, 26].

However, understanding what really happens inside a CapsNet is still an open challenge. Indeed, for a given input image, there are too many active (and each-other coupled) capsules, making the routing algorithm connections still difficult to understand, as the coupling coefficients typically have each-other similar values (Fig. 1), non exploiting the routing algorithm potential and making architectures without routing performing comparably [3]. Furthermore, backward and forward passes of a CapsNet come at an enormous computational cost, since the number of trainable parameters is very high. For example, the CapsNet model deployed on the MNIST dataset by Sabour et al. [21] is composed by an encoder and a decoder part. The full architecture has 8.2M of parameters. Do we really need that amount of trainable parameters to achieve competitive results on such

a task? Recently, many pruning methods were applied to CNNs in order to reduce the complexity of the networks, enforcing sparse topologies [13, 14, 24]: is it possible to tailor one of these approaches with not only the purpose of lowering the parameters, but aiding the model’s interpretability?

This work introduces REM (Routing Entropy Minimization) for CapsNets, which aims to improve the explainability of the routing algorithm of CapsNets. Pruning can effectively reduce the overall entropy of the connections of the parse tree-like structure encoded in a CapsNet, because in low pruning regimes it removes noisy couplings which cause the entropy to increase considerably. We collect the coupling coefficients studying their frequency and cardinality, observing lower per-class conditional entropy on these: the pruned version adds a missing explicit prior in the routing mechanism, grounding the coupling of the unused primary capsules disallowing fluctuations under the same baseline performance on the validation/test set. This implies that the parse trees are more stable for the pruned models, providing higher explainability on the relevant features (per-class) selected from the routing mechanism.

This paper is organized as follows: in Section 2 we introduce some of the basic concepts of CapsNets and their related works, in Section 3 we describe our technique called REM, in Section 4 we investigate the effectiveness of our method testing it on many datasets. The last two sections discuss the limitations of our approach and the conclusion of our work.

2. Background and Related Work

This section first describes the fundamental aspects of CapsNets and their routing algorithm introduced by [21]. Then, we review the literature especially related to how introduce sparsity into CapsNets. The notation used in our work is summarized in Table 1.

Capsule Networks Fundamentals. CapsNets group neurons into *capsules*, namely activity vectors, where each capsule accounts for an object of one of its parts. Each element of these vectors accounts for different properties of the object such as its pose and other properties like color,

Symbols	Meaning
Ξ	Cardinality of the dataset
M, N	Spatial dimensions of the PrimaryCaps layer
T	Primary capsules types
I	Primary capsules
J	Output (digit) capsules
\hat{y}^ξ	Target class for the ξ -th sample
y^ξ	Predicted class for the ξ -th sample
θ	Generic parameter for the model
\mathbf{u}_i	Pose of the i -th primary capsule (normalized)
\mathbf{s}_j	Pose of the j -th output capsule (non-normalized)
\mathbf{v}_j	Pose of the j -th output capsule (normalized)
c_{ij}^ξ	Coupling coefficient for the ξ -th input linking the i -th primary capsule to the j -th output capsule
\mathbf{c}_{-j}	Couplings to the same j -th output caps
\mathbf{W}	Transformation matrix
$\mathbb{1}_{y^\xi}$	One-hot encoding for the target class y^ξ
$\Theta(\cdot)$	One-step function
$q_K(\cdot)$	Uniform quantizer on K levels
\hat{x}	Quantized representation of x
$\mathbb{P}(x)$	Probability of x
\mathbb{H}_j	Entropy of the couplings toward j -th output capsule
\mathbb{H}	Entropy of the couplings for the CapsNet

Table 1. Summary of the notation.

deformation, etc. [21]. The magnitude of a capsule stands for the probability of existence of that object in the image [21]. Fig. 2 shows a standard architecture of a CapsNet with two capsule layers, PrimaryCaps and DigitCaps (also called OutputCaps). The poses of L -th capsules \mathbf{u}_i , called *primary capsules*, are built upon convolutional layers. In order to compute the poses of the capsules of the next layer $L + 1$, an iterative routing mechanism is performed. Each capsule \mathbf{u}_i makes a prediction $\hat{\mathbf{u}}_{j|i}$, thanks to a transformation matrix \mathbf{W}_{ij} , for the pose of an upper layer capsule j

$$\hat{\mathbf{u}}_{j|i} = \mathbf{W}_{ij}\mathbf{u}_i. \tag{1}$$

Then, the total input \mathbf{s}_j of capsule j of the DigitCaps

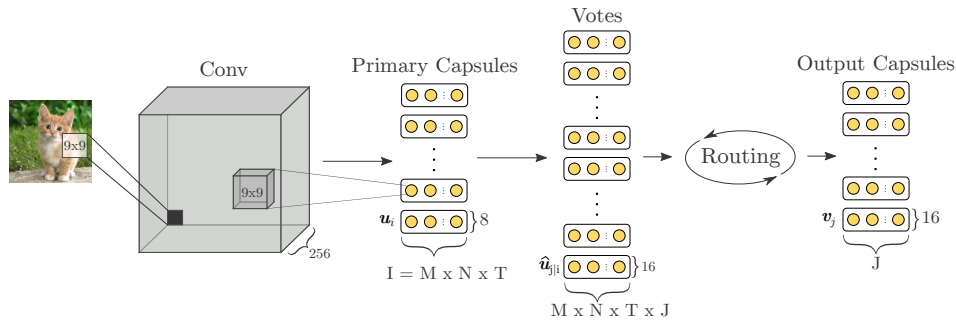


Figure 2. Capsule Network architecture (encoder network).

layer is computed as the weighted average of votes $\hat{\mathbf{u}}_{j|i}$

$$\mathbf{s}_j = \sum_i c_{ij} \hat{\mathbf{u}}_{j|i}, \quad (2)$$

where c_{ij} are the coupling coefficients between a primary capsule i and an output capsule j . The pose \mathbf{v}_j of an output capsule j is then defined as the normalized ‘‘squashed’’ \mathbf{s}_j

$$\mathbf{v}_j = \text{squash}(\mathbf{s}_j) = \frac{\|\mathbf{s}_j\|^2}{1 + \|\mathbf{s}_j\|^2} \frac{\mathbf{s}_j}{\|\mathbf{s}_j\|}. \quad (3)$$

So the routing algorithm computes the poses of output capsules and the connections between capsules of consecutive layers. The coupling coefficients are computed dynamically by the routing algorithm and they are dependent on the input [21]. The coupling coefficients are determined by a ‘‘routing softmax’’ activation function, whose initial logits b_{ij} are the log prior probabilities the i -th capsule should be coupled to the j -th one

$$c_{ij} = \text{softmax}(b_{ij}) = \frac{e^{b_{ij}}}{\sum_k e^{b_{ik}}} \quad (4)$$

At the first step of the routing algorithm they are equals and then they are refined by measuring the agreement between the output \mathbf{v}_j of the j -th capsule and the prediction $\hat{\mathbf{u}}_{j|i}$ for a given input. The agreement is defined as the scalar product $a_{ij} = \mathbf{v}_j \cdot \hat{\mathbf{u}}_{j|i}$. At each iteration, the update rule for the logits is

$$b_{ij} \leftarrow b_{ij} + a_{ij}. \quad (5)$$

The steps defined in (2), (3), (4), (5) are repeated for the t iterations of the routing algorithm. In order to train the network, Sabour *et al.* [21] replaced the cross entropy loss with the *margin loss*.

2.1. Related work

Capsule Networks. They were first introduced by Sabour *et al.* [21] and since then a lot of work has been done, both to improve the routing mechanism and to build deeper models. Regarding the routing algorithm, Hinton *et al.* [6] replace the dynamic routing with Expectation-Maximization, adopting matrix capsules instead of vector capsules. Wang *et al.* [25] model the routing strategy as an optimization problem. Li *et al.* [11] use master and aide branches to reduce the complexity of the routing process. Hahn *et al.* [5] incorporates a *self-routing* method such that capsule models do not require agreements anymore. De Sousa Ribeiro *et al.* [2] replace the routing algorithm with variational inference of part-object connections in a probabilistic capsule network, leading to a significant speedup without sacrificing performance. Since the

CapsNet model introduced by Sabour *et al.* [21] is a shallow network, several works attempted to build deep CapsNets. Rajasegaran *et al.* [18] propose a deep capsule network architecture which uses a novel 3D convolution based dynamic routing algorithm aiming at improving the performance of CapsNets for more complex image datasets. Guglberger *et al.* [4] introduce residual connections to train deeper capsule networks.

Sparse Capsule Networks. A naive solution to reduce uncertainty within the routing algorithm is to simply running more iterations. As shown by Paik *et al.* [16] and Gu *et al.* [3], the routing algorithms tends to overly polarize the link strengths, namely a simple route in which each input capsule sends its output to only one capsule and all other routes are suppressed. On the one hand, this behavior is desirable because it makes the routing algorithm more explainable, by making it possible to extract a parse tree thanks to this coupling coefficients. On the other hand, running many iterations is only useful in the case of networks with few parameters, as demonstrated by Renzulli *et al.* [20], otherwise the performance will drop. Rawlinson *et al.* [19] trained CapsNets in an unsupervised setting, showing that in unsupervised learning the routing algorithm does not discriminate among capsule anymore: the coupling coefficients collapse to the same value. Therefore, they sparsify latent capsule layers activities by masking output capsules according to a custom ranking function. Kosiorek *et al.* [9] impose sparsity and entropy constraints into capsules, but they do not employ an iterative routing mechanism. Jeong *et al.* [7] introduced a structured pruning layer called ladder capsule layers, which removes irrelevant capsules, namely capsules with low activities. Kakioglu *et al.* [8] solve the task of 3D object classification on point clouds with pruned Capsule Networks. Their objective was to compress robust capsule models in order to deploy them on resource-constrained devices.

The main contribution of our work relies on the fact that we regularize and prune the parameters in a CapsNet as a way to minimize the entropy of the connections computed by the routing algorithm. In fact, we show that relationships between objects and their parts in a standard CapsNets described by Sabour *et al.* [21] have high entropies. We minimize these entropies so that we can extract stronger parse trees. This allows us to effectively build dictionaries upon the input datasets and understand which are the shared object parts and transformations between different the entities in the images.

3. Routing Entropy Minimization

The coupling coefficients computed by the routing mechanism model the part-whole relationships between capsules of two consecutive capsule layers, as displayed in Fig. 1. Assigning parts to objects (namely learning how

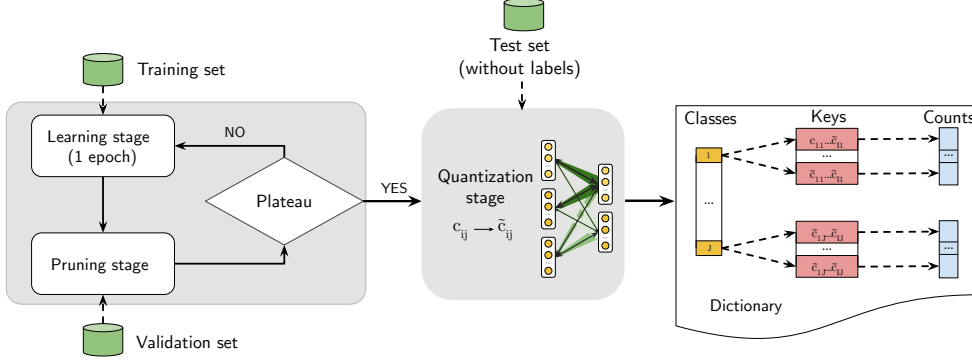


Figure 3. Pipeline of REM.

each object is composed), is a challenging task. One of the main goal of the routing algorithm is to extract a parse tree of these relationships. Given the ξ -th input of class j , an ideal parse tree for a primary capsule i detecting one of the parts of the entity in the input ξ would ideally lead to

$$c_{i-}^{\xi} = \mathbb{1}_{j^{\xi}}. \quad (6)$$

This means that the routing process is able to carve a parse tree out of the CapsNet which explains perfectly the relationships between parts and wholes. One of the problems of this routing procedure is that there is no constraint on how strong a parse tree should be. In this section we present our technique REM, first showing how to extract a parse tree and then how to build stronger parse trees. The pipeline of our method is depicted in Fig. 3.

3.1. Parse trees extraction

Once we have a trained CapsNets model, in order to interpret the routing mechanism, we extract all the possible routing coupling coefficients and build a parse tree. Towards this end, we want to define a metric which helps us deciding if the relationships captured by the routing algorithm resemble or not a parse tree. Therefore, we organize the coupling coefficients into *associative arrays*, we can compute the number of occurrences of each coupling sequence in order to compute the entropy of the whole coupling dictionary to measure the simplicity of the parse tree. In the next paragraphs, we explain how to generate these sequences by discretizing the coupling coefficients and how to create the dictionary.

Quantization. During the quantization stage, we first compute the *continuous* coupling coefficients c_{ij}^{ξ} for each ξ -th input example. It should be noticed that c_{ij}^{ξ} are the coupling coefficients obtained after the forward pass of the last routing iteration. Then, we quantize every c_{ij}^{ξ} into K discrete levels through the uniform quantizer $q_K(\cdot)$, obtaining

$$\tilde{c}_{ij}^{\xi} = q_K(c_{ij}^{\xi}). \quad (7)$$

We choose the lowest K such that the accuracy is not deteriorated. We will here on refer to CapsNet+Q as trained CapsNet where the coupling coefficients are quantized.

Extracting the parse tree. Given the quantized coupling coefficients of a CapsNet+Q, we can extract the parse tree (and create a dictionary of parse trees) for each class j , where each entry is a string composed by the quantization indices of the coupling coefficients. We will extract the coupling coefficients \tilde{c}_{-j}^{ξ} between the primary capsules I and the predicted j -th output capsule. Given a dictionary for the coupling coefficients of a CapsNet+Q, we can compute the entropy for each class as

$$\mathbb{H}_j = - \sum_{\xi} \left\{ \mathbb{P}(\tilde{c}_{-j}^{\xi} | y^{\xi} = j) \cdot \log_2 \left[\mathbb{P}(\tilde{c}_{-j}^{\xi} | y^{\xi} = j) \right] \right\} \quad (8)$$

where $\mathbb{P}(\tilde{c}_{-j}^{\xi} | y^{\xi} = j)$ is the frequency of occurrences of a generic string ξ for each *predicted* class y^{ξ} . Finally, the entropy of a dictionary for a CapsNet+Q on a given dataset is the average of the entropies H_j of each class

$$\mathbb{H} = \frac{1}{J} \sum_j \mathbb{H}_j. \quad (9)$$

Intuitively, the lower (9), the stronger the connections between capsules are in the parse tree-like structure carved-out from the routing algorithm. We also target to obtain the distribution of these coupling coefficients. In general, we know we have $\Xi \times I \times J$ coupling coefficients for the full dataset (with potential redundancies). Given the i -th primary capsule, however, we are only interested to $c_{-j}^{\xi} | y^{\xi} = j$. In this way, we reduce the coupling coefficients space to $I \times J$. We compute then the average of all the inputs belonging to an object class in order to output just $I \times J$ coupling coefficients.

Preliminary result. Let us now generate the parse trees on the CapsNet model trained on the MNIST dataset as in [21], investigating their evolution during training. To this end, we compute the distribution of the coupling coefficients on the test set for two models: the model trained

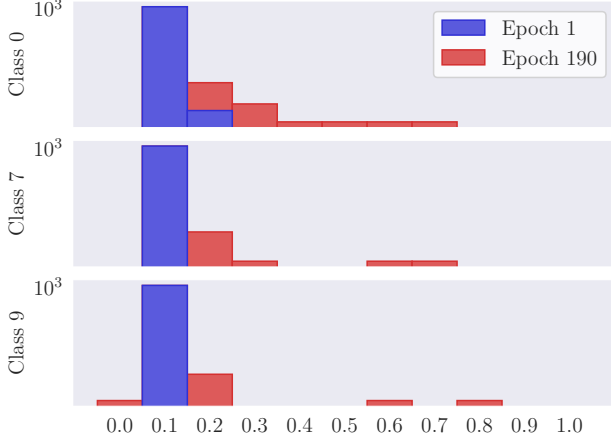


Figure 4. Coupling coefficients distributions of two CapsNets+Q at epochs 1 and 190 on MNIST (test set).

Model	Accuracy	Entropy
CapsNet ₁ +Q	97.53	1.83
CapsNet ₁₉₀ +Q	99.55	9.41

Table 2. Classification results (%) and entropy of two CapsNets+Q at epochs 1 and 190 on MNIST (test set).

after the first epoch and the one that achieved the lowest loss value on the validation set. Fig. 4 shows the distributions for the two models and Table 2 reports the corresponding accuracy and entropy values. We sampled a subset of the distributions for all the object classes. It can be observed that after the first epoch CapsNet is clearly far from optimality, both in term of performance and parse tree explainability: indeed all coupling coefficients are almost all equals to the value selected at initialization, i.e. $1/J$. This effect is almost the same when we train a CapsNet with $t = 1$ as Gu et al. [3], where its entropy is exactly zero but capsules are uniformly coupled. On the other hand, a well trained CapsNet achieves higher generalization but its entropy is getting higher, so the routing mechanism is difficult to interpret and to explain. As a matter of fact, we can see in Table 3 the dictionary for the CapsNet₁₉₀+Q: the number of keys for each class is too high to make the routing algorithm explainable. Notice that the MNIST test set has 10k images and the total number of keys is 8147. We target a model that has high generalization but a dictionary where number of keys is low.

3.2. Unconstrained routing entropy

In this subsection we are going to more-formally analyze the distribution of the coupling coefficients

$$c_{ij} = \frac{e^{b_{ij} + \sum_{r=1}^t v_j^r u_j \mathbf{W}_{ij}}}{\sum_k e^{b_{ik} + \sum_{r=1}^t v_k^r u_k \mathbf{W}_{ik}}} \quad (10)$$

where t indicates the target routing iterations.¹ Let us evaluate the c_{ij} over a non-yet trained model: as we saw also in Section 3.1, we have

$$c_{ij} \approx \frac{1}{J} \forall i, j. \quad (11)$$

When updating the parameters, following [3], we have

$$\frac{\partial L}{\partial \mathbf{W}_{ij}} = \left[\frac{\partial L}{\partial v_j} \frac{\partial v_j}{\partial s_j} \cdot c_{ij} + \sum_{m=1}^M \left(\frac{\partial L}{\partial v_m} \frac{\partial v_m}{\partial s_m} \cdot \hat{u}_{m|i} \frac{\partial c_{im}}{\partial \hat{u}_{m|i}} \right) \right] \cdot \mathbf{u}_i \quad (12)$$

where we can have the gradient for $\mathbf{W}_{ij} \approx 0$ in a potentially-high number of scenarios, despite $c_{ij} \neq \{0, 1\}$. Let us analyze the simple case in which we have perfect outputs, matching the ground truth, hence we are close to a local (or potentially the global) minimum of the loss function:

$$\left\| \frac{\partial L}{\partial v_m} \right\|_2 \approx 0 \forall m. \quad (13)$$

Looking at (4), we see that the right class is chosen, but given the squashing function, we have as an explicit constraint that, given the j -th class as the target one, we require

$$\|\mathbf{v}_j\|_2 \gg \|\mathbf{v}_m\|_2 \quad \forall m \neq j \quad (14)$$

on the \mathbf{W}_{ij} , which can be accomplished in many ways, including:

- having sparse activation for the primary capsules \mathbf{u}_i : in this case, we have constant \mathbf{W}_{ij} (typically associated to no-routing based approaches); however, we need heavier deep neural networks as they have to force sparse signals already at the output of the primary capsules. In this case, the coupling coefficients c_{ij} are also constant by definition;
- having sparse votes $\hat{u}_{j|i}$: this is a combination of having both primary capsules and weights \mathbf{W}_{ij} enforcing sparsity in the votes, and the typical scenario with many routing iterations.

Having sparse votes, however, does not necessarily result in having sparse coupling coefficients: according to (5), the coupling coefficients are multiplied with the votes, obtaining the output capsules. The distribution of the coupling coefficients requires (14) to be satisfied only: if \mathbf{W}_{ij} is not sparsely distributed, we can still have sparse votes. However, this is the main reason we observe high entropy in the coupling coefficient distributions (Fig. 4): as the votes $\hat{u}_{j|i}$ are implicitly sparse (yet also disordered, as we are not explicitly imposing any structure in the coupling coefficients

¹for abuse of notation, in this subsection we suppress the index ξ

Model	# ₀	# ₁	# ₂	# ₃	# ₄	# ₅	# ₆	# ₇	# ₈	# ₉
CapsNet ₁₉₀ +Q	974	358	968	967	859	856	939	670	965	591

Table 3. Dictionary sizes for the CapsNet₁₉₀+Q model on MNIST (test set).

distribution), the model is still able to learn but it finds a typical solution where c_{ij} are not sparse. However, we would like to have sparsely distributed, recurrent c_{-j} , establishing stable relationships between the features extracted at primary capsules layer.

Minimizing explicitly the entropy term (8) is an intractable problem due to the non-differentiability of the entropy term and of the quantization step (in our considered setup) and due to the huge computational complexity to be introduced at training time. Hence, we can try to implicitly enforce routing entropy minimization by forcing a sparse and organized structure in the coupling coefficients. Towards this end, one efficient solution relies in enforcing sparsity in the \mathbf{W}_{ij} representation: enforcing a vote between the i -th primary capsule and the j -th output caps to be exactly zero for any input, according to (10)

$$c_{ij} = \frac{1}{\sum_k e^{b_{ik} + \sum_{r=1}^t v_r^i \mathbf{u}_k \mathbf{W}_{ik}}}. \quad (15)$$

In this way, having a lower variability in the c_{ij} values (and hence building more stable relationships between primary and output capsules), straightforwardly we are also explicitly minimizing the entropy of the quantized representations for the coupling coefficients. In the next subsection, we are going to tailor a sparsity technique to accomplish such a goal.

3.3. Enforcing REM with pruning

CapsNets are trained via standard back-propagation learning, minimizing some loss function like margin loss. Our ultimate goal is to assess to which extent a variation of the value of some parameter θ would affect the error on the network output. In particular, the parameters not affecting the network output can be pushed to zero in a soft manner, meaning that we can apply an ℓ_2 penalty term. A number of approaches have been proposed, especially in the recent years [10, 12, 15]. One recent state-of-the-art approach, LOBSTER [23] proposes to penalize the parameters by their gradient-weighted ℓ_2 norm, leading to the update rule

$$\theta^{t+1} = \theta^t - \eta G \left[\frac{\partial L}{\partial \theta^t} \right] - \lambda \theta^t \text{ReLU} \left[1 - \left| \frac{\partial L}{\partial \theta^t} \right| \right], \quad (16)$$

where $G \left[\frac{\partial L}{\partial \theta^t} \right]$ is any gradient-based optimization update (for SGD it is the plain gradient, but other optimization strategies like Adam can be plugged) and η, λ are two positive hyper-parameters.

Such a strategy is particularly effective on standard convolutional neural networks, and easy to plug in any back-propagation based learning system. Furthermore, LOBSTER is a regularization strategy which can be plugged at any learning stage, as it self-tunes the penalty introduced according to the learning phase: for this non-intrusiveness in the complex and delicate routing mechanism for CapsNets, it resulted a fair choice to enforce REM.

4. Experiments and Results

In this section we report the experiments and the results that we performed to test REM. We first show the results on the MNIST dataset, reporting also how the entropy and the accuracy values change during training. Then, we test REM on more complex datasets such as Fashion-MNIST, CIFAR10 and Tiny ImageNet. We also performed experiments to test the robustness to affine transformations of CapsNets+REM. Except for Tiny ImageNet, we used the same architectures configurations and augmentations described in [21].² We trained models with five random seeds. We report the classification accuracy (%) and entropy (averages and standard deviations), the *sparsity* (percentage of pruned parameters, median) and the number of keys in the dictionary (median). The code will be open-source released upon acceptance of the paper, to guarantee the reproducibility of the results. The experiments were run on a Nvidia Ampere A40 equipped with 48GB RAM, and the code uses PyTorch 1.9.

4.1. Preliminary results on MNIST

In order to assess our REM technique, we analyze in-depth the benefits of pruning towards REM on the MNIST dataset. Nowadays, despite its outdatedness, MNIST remains an omni-present benchmark for CapsNets [3, 19, 21]. Fig. 5 shows how the entropy (red line) and classification accuracy (blue dotted line) changes as the sparsity increases during training. We can see that at the beginning of the training stage the entropy is low because the routing algorithm has not learned yet to correctly discriminate the relationships between the capsules; but at the end of the training process REM lowers the entropy of the network. In Fig. 6 we plot the distributions of the coupling coefficients for a CapsNet+Q and a CapsNet+REM following the method described in Sec. 3.1. We can see that the distributions of the CapsNet+REM model are sparser than the ones for the

²we have removed the decoder part of the network, see Sec. 4.3 for more details.

Model	Accuracy	Sparsity
CapsNet	99.57±0.0002	0
CapsNet	99.58±0.0003	85.53
CapsNet+Q	99.56±0.0003	0
CapsNet+REM	99.56±0.0002	85.53

Table 4. Results for CapsNets, CapsNets+Q, CapsNets+REM on MNIST (test set).

Model	Sparsity	# ₀	# ₁	# ₂	# ₃	# ₄	# ₅	# ₆	# ₇	# ₈	# ₉	Entropy
CapsNet+Q	0	972	489	1007	985	904	856	939	670	968	957	9.53±0.54
CapsNet+REM	85.53	40	46	15	39	12	117	182	14	310	9	4.16±1.59

Table 5. (Quantized) CapsNets number of keys for each class on MNIST (test set).

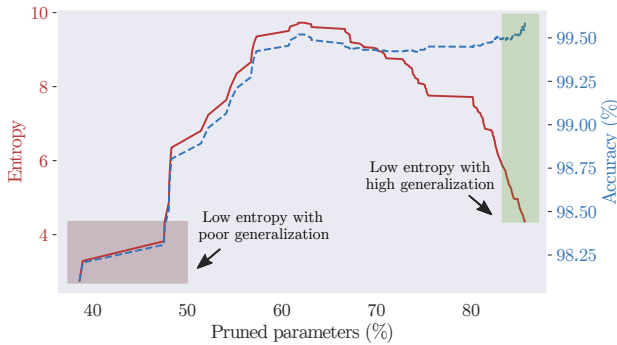


Figure 5. Accuracy and entropy curves vs pruned parameters on MNIST (test set).

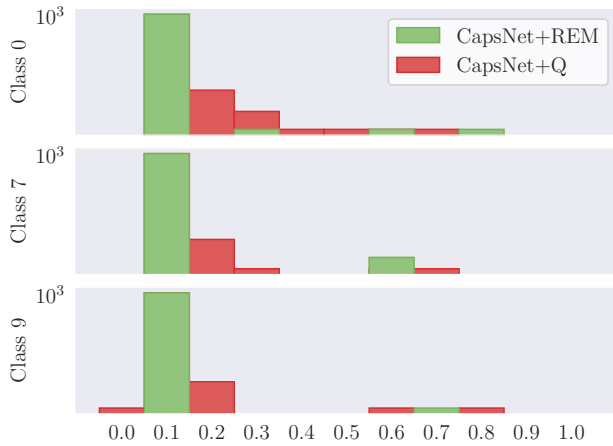


Figure 6. Coupling coefficients distributions for each class of a CapsNet+Q and a CapsNet+REM on MNIST (test set).

CapsNet+Q model, namely we carve a stronger parse tree while achieving high generalization. Table 4 shows that there is no performance loss when pruning a CapsNet, even when REM is applied with its quantization levels. Table 5 shows the number of keys in each class for CapsNet+REM and a CapsNet+Q, namely a CapsNet where the quantization is applied without pruning the network during train-



Figure 7. Each digit is a cluster composed by the input images. Shared object parts and transformations are extracted with the dictionary of a CapsNet+REM.

ing. We also report the number of keys for each class and the entropy of the dictionary for the same quantized models shown in Table 4. We can see that the dimension of the dictionary for CapsNet+REM is lower than the one for CapsNet+Q. Also the entropy measure for CapsNet+REM is lower compared to CapsNet+Q, namely, REM has successfully built a parse tree between primary and class capsules with stronger relationships. We now show how we can improve the explainability of such connections. Each key can be seen as a *cluster* of images with shared features or parts. For each key of the predicted class, we take all the images of the input dataset that belong to that key, sorted according to the size of that cluster. Then, we overlap all the images in a cluster. Figure 7 depicts a visual representation of some of these clusters for a subset of object classes. We can see that a CapsNet+REM can not only predict which digit is present in an input image, but it can also show which are the shared object parts (such as different localized parts for the digit 7 and 9) and their transformations (rotation and translation for the digit 0) in a cluster.

4.2. Results

We trained and tested CapsNet+REM on more complex datasets such as:

- Fashion-MNIST, 28x28 grayscale images (10 classes);
- CIFAR10, 32x32 RGB images (10 classes);
- Tiny ImageNet, 64x64 RGB images (200 classes).

Model	F-MNIST			CIFAR10			T-ImageNet		
	Accuracy	Sparsity	Entropy	Accuracy	Sparsity	Entropy	Accuracy	Sparsity	Entropy
CapsNet+Q	92.46±0.002	0	8.64±1.15	78.42±0.026	0	6.26±0.61	58.50±0.25	0	5.18±0.67
CapsNet+REM	92.62±0.001	80.71	4.80±1.70	79.25±0.005	81.17	4.15±0.62	54.02±0.14	44.27	3.15±0.81

Table 6. Accuracy, sparsity and entropy results on on Fashion-MNIST, CIFAR10 and Tiny ImageNet (test set).

Model	expanded MNIST		affNIST	
	Accuracy	Accuracy	Sparsity	Entropy
CapsNet+Q	99.22	77.93±0.005	0	8.64±1.15
CapsNet+REM	99.22	81.81±0.008	71.26	8.45±1.10
CapsNet+Q	99.36±0.0005	83.14±0.002	0	8.45±0.99
CapsNet+REM	99.48±0.0002	85.23±0.001	87.32	5.93±1.39

Table 7. Accuracy, sparsity and entropy results on affNIST test set for under and well-trained models.

Specific setup for Tiny ImageNet. In order to test also in transfer learning scenarios, we train CapsNets on the Tiny ImageNet dataset, using in this case only a pretrained ResNet18 model as back-bone and fine-tuning the CapsNet parameters only. We used 10% of the training set as validation set and the original validation set as test set.

Discussion. As we can see in Tables 6, a CapsNet+REM has an high percentage of pruned parameters with a minimal performance loss. So this confirms our hypothesis that CapsNets are over-parametrized. Furthermore, for the Fashion-MNIST dataset the entropy of the CapsNet+REM is much lower than the CapsNet+Q, while for the other datasets the differences between the two approaches is less evident. This is an expected behavior: for CIFAR10 and Tiny ImageNet, both CapsNets achieved poor classification results and this introduces noise on the coupling coefficients, leading to higher uncertainty in the classification task hence in the features selection.

Robustness to affine transformations. To test the robustness to affine transformations of CapsNets+REM, we used expanded MNIST: a dataset composed by padded and translated MNIST, in which each example is an MNIST digit placed randomly on a black background of 40×40 pixels. We used the affNIST dataset as test set, in which each example is an MNIST digit with a random small affine transformation. We tested an under-trained CapsNet with early stopping which achieved 99.22% accuracy on the expanded MNIST test set as in [3, 21]. We also trained these models until convergence. We can see in Table 7 that the under-trained networks entropies are high. Instead, a well-trained CapsNet+REM can be robust to affine transformations and have a low entropy.

4.3. Limitation

A CapsNet is typically composed of an encoder and a decoder part, where the latter is a reconstruction network with 3 fully connected layers [21]. In the previously-discussed experiments, we have removed the decoder. The main lim-

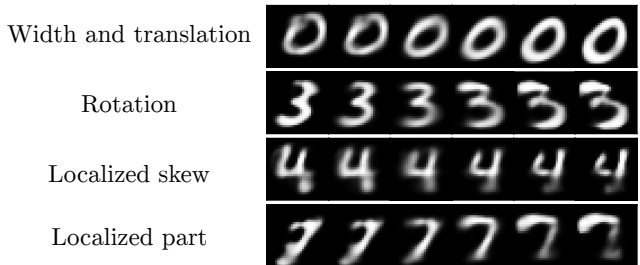


Figure 8. MNIST perturbation reconstructions of a frozen CapsNet+REM with a decoder stacked on top of it.

itation of our work arise when computing the entropy of CapsNets trained with the decoder. We observed that the entropy of a CapsNets+REM is almost the same as that of a CapsNet+Q shown in Tables 5 and 6. Indeed, when the decoder is used, the activity vector of an output capsule encodes richer representations of the input. Sabour *et al.* [21] introduced the decoder to boost the routing performance on MNIST by enforcing the pose encoding a capsule. They also show that, when a perturbed activity vector is feeded to the decoder, such perturbation affects the reconstruction. So capsules representations are *equivariant*, meaning that transformations applied to the input are described by continuous changes in the output vector. In order to verify if output capsules of a trained CapsNet+REM without the decoder (so with low entropy) are still equivariant, we stacked on top of it the reconstruction network, without training the encoder. We can see in Fig. 8 that the output capsules are still equivariant to many transformations so we successfully obtained a CapsNet+REM with low entropy but with equivariant representations encoded into capsules.

5. Conclusion

This paper investigated and improved the explainability of the routing algorithm in CapsNets with REM (Routing Entropy Minimization), which drives the model parameters

distribution towards low entropy configurations. We first showed how to extract the parse tree of a CapsNet by discretizing its connections and then collecting the possible parse trees in associative arrays. Standard CapsNets show high entropy in the parse trees structures, as an explicit prior on the coupling coefficients distribution is missing. We showed how pruning methods, in low pruning regimes, naturally reduce such entropy as well as the cardinality over the possible parse trees, testing such a phenomenon on several datasets. Furthermore, we empirically observe that a CapsNet+REM model remains robust to affine transformations and its output capsules are still equivariant. REM opens research pathways towards the distillation of parse trees and model interpretability, including the design of a pruning technique specifically-designed for REM.

References

- [1] Parnian Afshar, Arash Mohammadi, and Konstantinos N Plataniotis. Brain tumor type classification via capsule networks. In *2018 25th IEEE International Conference on Image Processing (ICIP)*, pages 3129–3133. IEEE, 2018. [1](#)
- [2] Fabio De Sousa Ribeiro, Georgios Leontidis, and Stefanos Kollias. Introducing routing uncertainty in capsule networks. In *Advances in Neural Information Processing Systems*, volume 33, pages 6490–6502. Curran Associates, Inc., 2020. [3](#)
- [3] Jindong Gu and Volker Tresp. Improving the robustness of capsule networks to image affine transformations. In *Proceedings of the IEEE/CVF Conference on Computer Vision and Pattern Recognition (CVPR)*, June 2020. [1](#), [3](#), [5](#), [6](#), [8](#)
- [4] Josef Gugglberger, David Peer, and Antonio Rodríguez-Sánchez. Training deep capsule networks with residual connections. In Igor Farkaš, Paolo Masulli, Sebastian Otte, and Stefan Wermter, editors, *Artificial Neural Networks and Machine Learning – ICANN 2021*, pages 541–552, Cham, 2021. Springer International Publishing. [3](#)
- [5] Taeyoung Hahn, Myeongjang Pyeon, and Gunhee Kim. Self-routing capsule networks. In *Advances in Neural Information Processing Systems*, volume 32, pages 7658–7667. Curran Associates, Inc., 2019. [3](#)
- [6] Geoffrey E Hinton, Sara Sabour, and Nicholas Frosst. Matrix capsules with EM routing. In *International Conference on Learning Representations*, 2018. [1](#), [3](#)
- [7] Taewon Jeong, Youngmin Lee, and Heeyoung Kim. Ladder capsule network. In Kamalika Chaudhuri and Ruslan Salakhutdinov, editors, *Proceedings of the 36th International Conference on Machine Learning*, volume 97 of *Proceedings of Machine Learning Research*, pages 3071–3079. PMLR, 09–15 Jun 2019. [3](#)
- [8] Burak Kakillioglu, Ao Ren, Yanzhi Wang, and Senem Velipasalar. 3d capsule networks for object classification with weight pruning. *IEEE Access*, 8:27393–27405, 2020. [3](#)
- [9] Adam Kosiorek, Sara Sabour, Yee Whye Teh, and Geoffrey E Hinton. Stacked capsule autoencoders. In *Advances in Neural Information Processing Systems*, volume 32, pages 15512–15522. Curran Associates, Inc., 2019. [1](#), [3](#)
- [10] Namhoon Lee, Thalaiyasingam Ajanthan, and Philip HS Torr. Snip: Single-shot network pruning based on connection sensitivity. *arXiv preprint arXiv:1810.02340*, 2018. [6](#)
- [11] Hongyang Li, Xiaoyang Guo, Bo Dai, Wanli Ouyang, and Xiaogang Wang. Neural network encapsulation. In *Computer Vision – ECCV 2018*, pages 266–282, Cham, 2018. Springer International Publishing. [3](#)
- [12] Christos Louizos, Max Welling, and Diederik P Kingma. Learning sparse neural networks through l_0 regularization. *arXiv preprint arXiv:1712.01312*, 2017. [6](#)
- [13] Christos Louizos, Max Welling, and Diederik P. Kingma. Learning sparse neural networks through l_0 regularization. In *Proceedings of the 6th International Conference on Learning Representations, ICLR*. OpenReview.net, 2018. [2](#)
- [14] Dmitry Molchanov, Arsenii Ashukha, and Dmitry Vetrov. Variational dropout sparsifies deep neural networks. In *Proceedings of the 34th International Conference on Machine Learning*, 2017. [2](#)
- [15] Pavlo Molchanov, Arun Mallya, Stephen Tyree, Iuri Frosio, and Jan Kautz. Importance estimation for neural network pruning. In *Proceedings of the IEEE/CVF Conference on Computer Vision and Pattern Recognition*, pages 11264–11272, 2019. [6](#)
- [16] Inyoung Paik, Taeyeong Kwak, and Injung Kim. Capsule networks need an improved routing algorithm. In *Proceedings of The Eleventh Asian Conference on Machine Learning*, volume 101 of *Proceedings of Machine Learning Research*, pages 489–502, Nagoya, Japan, 17–19 Nov 2019. PMLR. [3](#)
- [17] Mercedes E Paoletti, Juan Mario Haut, Ruben Fernandez-Beltran, Javier Plaza, Antonio Plaza, Jun Li, and Filiberto Pla. Capsule networks for hyperspectral image classification. *IEEE Transactions on Geoscience and Remote Sensing*, 57(4):2145–2160, 2018. [1](#)
- [18] J. Rajasegaran, V. Jayasundara, S. Jayasekara, H. Jayasekara, S. Seneviratne, and R. Rodrigo. Deepcaps: Going deeper with capsule networks. In *2019 IEEE/CVF Conference on Computer Vision and Pattern Recognition (CVPR)*, pages 10717–10725, 2019. [3](#)
- [19] David Rawlinson, Abdelrahman Ahmed, and Gideon Kowadlo. Sparse unsupervised capsules generalize better. *CoRR*, abs/1804.06094, 2018. [3](#), [6](#)
- [20] Riccardo Renzulli, Enzo Tartaglione, Attilio Fiandrotti, and Marco Grangetto. Capsule networks with routing annealing. In Igor Farkaš, Paolo Masulli, Sebastian Otte, and Stefan Wermter, editors, *Artificial Neural Networks and Machine Learning – ICANN 2021*, pages 529–540, Cham, 2021. Springer International Publishing. [3](#)
- [21] Sara Sabour, Nicholas Frosst, and Geoffrey E Hinton. Dynamic routing between capsules. In *Advances in Neural Information Processing Systems*, volume 30, pages 3856–3866. Curran Associates, Inc., 2017. [1](#), [2](#), [3](#), [4](#), [6](#), [8](#)
- [22] Ramprasaath R. Selvaraju, Michael Cogswell, Abhishek Das, Ramakrishna Vedantam, Devi Parikh, and Dhruv Batra. Grad-cam: Visual explanations from deep networks via gradient-based localization. In *2017 IEEE International Conference on Computer Vision (ICCV)*, pages 618–626, 2017. [1](#)

- [23] Enzo Tartaglione, Andrea Bragagnolo, Attilio Fiandrotti, and Marco Grangetto. Loss-based sensitivity regularization: towards deep sparse neural networks. *CoRR*, abs/2011.09905, 2020. [6](#)
- [24] Enzo Tartaglione, Skjalg Lepsø y, Attilio Fiandrotti, and Gianluca Francini. Learning sparse neural networks via sensitivity-driven regularization. In S. Bengio, H. Wallach, H. Larochelle, K. Grauman, N. Cesa-Bianchi, and R. Garnett, editors, *Advances in Neural Information Processing Systems*, volume 31. Curran Associates, Inc., 2018. [2](#)
- [25] Dilin Wang and Q. Liu. An optimization view on dynamic routing between capsules. In *ICLR*, 2018. [3](#)
- [26] Yongheng Zhao, Tolga Birdal, Haowen Deng, and Federico Tombari. 3d point capsule networks. In *Proceedings of the IEEE/CVF Conference on Computer Vision and Pattern Recognition*, pages 1009–1018, 2019. [1](#)